Science Press

Trans. Nonferrous Met. Soc. China 17(2007) s818−s822

Transactions of Nonferrous Metals Society of China

www.csu.edu.cn/ysxb/

Effect of tension deformation on microstructure and mechanism of electrodeposited nickel coating

MA Zeng-sheng(马增胜), LONG Shi-guo(龙士国), ZHANG Xiao-bing(张小兵), PAN Yong(潘　勇), ZHOU Yi-chun(周益春)

Key Laboratory of Low Dimensional Materials & Application Technology, Ministry of Education, Faculty of Materials Optoelectronics & Physics, Xiangtan University, Xiangtan 411105, China

Received 15 July 2007; accepted 10 September 2007

Abstract: Nickel coating deposits with better ductility on a lower carbon steel sheet were produced by electrodeposition method and the electrodeposited nickel coating was deformed with the strain of 10%. Then the surface morphology, the deformation texture and the mechanical properties were analyzed by scanning electron microscopy (SEM), X-ray diffractometry (XRD) and nano-indentation measurement, respectively. The principle of nano-indentation to measure the hardness and elastic modulus of nickel coating was introduced. The relation curves of the load and displacement were obtained, including the original electrodeposited samples and the samples under tension. The results show that: 1) there are only two main texture components Ni (111) and Ni (200) in the nickel coating, and no new texture component is found due to the elongation; 2) after tensile deformation in the coating, the surface roughness increases and the microcrack is found; 3) The hardness and the elastic modulus decrease after tensile deformation; and 4) for the original electrodeposited sample, the indentation depths change with the load, the hardness and the elastic modulus decrease with the increase of the depth. In addition, the investigation of creep shows that the value of creep increases when the tensile strain $\varepsilon>10\%$.

Key words: electrodeposited nickel coating; tension deformation; nano-indentation; creep

1 Introduction

The nickel electrodeposited carbon steel sheet can be prepared by bilaterally electrodepositing nickel on low carbon steel sheet and its thickness is 1−20 μm. The grain size is in micrometer or nanometer [1−2]. The electrodeposited nickel coating becomes an important engineering material. It is found that this material has good corrosion resistance, attractive toughness and excellent plasticity, which offers the potential for advanced structure applications. In addition, the adhesion strength of electrodeposited nickel coating to substrates is excellent for their successful performance [3−4].

With the development of this material, the processing technique that the nickel is firstly electrodeposited on the steel substrate and then the coating and substrate are wholly formed is put forward instead of the process technique that the steel is firstly formed and then the production surface is electrodeposited by nickel coating. Therefore, the formation of sheet with coating is an important process technology [5−6]. However, it needs multi-procedure deformations to form a design shape. The pre-procedure shape deformation can significantly affect the post-procedure shape deformation. Therefore, to study the evolution of the microstructure and mechanism of the coating is necessary.

In this work, the effect of tension deformation on the micro-structure and mechanism, such as hardness, elastic modulus and creep of electrodeposited nickel coating were experimentally studied by SEM, XRD and nano-indentation methods.

2 Nano-indentation analysis technique

Fig.1 shows the typical load—displacement curve, obtained by the Oliver and Pharr method. Where h_f is the final unloading depth, h_{max} is the maximum loading depth during indentation tests, and P_{max} is the maximum

Foundation item: Project(104014) supported by Fok Ying Tong Education Foundation of Ministry of Education; project(05B008) supported by Scientific Research Fund of Hunan Provincial Education Department

Corresponding author: LONG Shi-guo; Tel: +86-732-8293577; E-mail: longsg@xtu.edu.cn

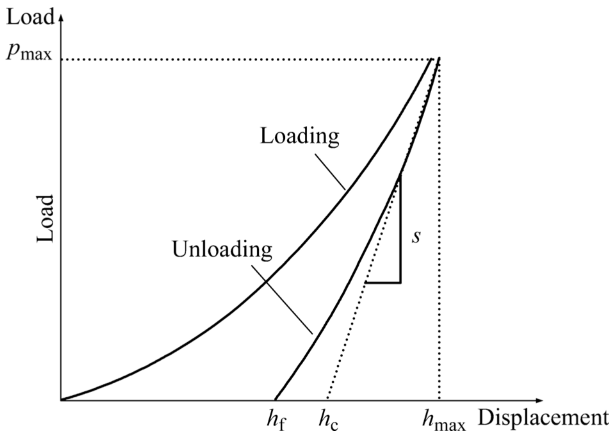

Fig.1 Schematic diagram of a nano-indentation load-displacement curve

load, s is the slope of the tangent line to the unloading curve at the maximum loading point (h_{max}, P_{max}) and is termed the system contact stiffness, h_c is the intercept value of the above mentioned tangent line down to P=0 and is termed the contact depth.

In nano-indentation, the reduced modulus, E_r, is given by

$$E_r = \frac{\sqrt{\pi}}{2}\frac{s}{\sqrt{A_c}} \tag{1}$$

Thus, the elastic Modulus, E, can be obtained from

$$\frac{1}{E_r} = \frac{1-\nu^2}{E} + \frac{1-\nu_i^2}{E_i} \tag{2}$$

where ν_i is aggregate Poisson ratio of the diamond indenter, 0.07 [7], and E_i is elastic modulus of the diamond indenter.

Among the methods for analyzing load-penetration depth data [8−10], the one proposed by OLIVER and PHARR is widely employed [1]. Their method assume that the relationship between penetration depth h and load P for some given indenter geometry can be represented as follows:

$$P = \alpha(h - h_f)^m \tag{3}$$

where α is a fitting parameter that contains geometric constants, elastic modulus and Poisson's ratio of the specimen and the indenter; m is a power law exponent related to the geometry of the indenter. For a fiat-ended cylindrical punch, m=1; for a paraboloid of revolution, m=1.5; and for a cone, m=2.

The system stiffness, s, as defined above, is given by

$$s = \left.\frac{dP}{dh}\right|_{h=h_{max}} = mA(h_{max} - h_f)^{m-1} \tag{4}$$

The contact depth h is given by

$$h_c = h_m - \varepsilon P_{max} / s \tag{5}$$

where ε is associated with the specific tip geometry. Once the contact depth is calculated, the contact area, A_c, can be obtained. For a perfect indenter, A_c is given by $A_c = 24.5h_c^2$. The hardness (H) can be defined as

$$H = \frac{P_{max}}{A_c} \tag{6}$$

3 Experimental

3.1 Coating specimen preparation and tensile experiment

A lower carbon steel sheet with thickness of 0.3 mm was used as substrate. A uniform nickel coating of thickness of 3 μm was prepared by electrodepositing method on both sides of the steel sheet. The coating was obtained with nickel sulphate electrolyte composed of 250 g/L $NiSO_4·6H_2O$, 50 g/L $NiCl_2·6H_2O$, 35 g/L H_3BO_3. Pure nickel was used as the anode. The pH value was adjusted with sulfuric acid to 4.0 at 42 ℃. A conventional rotating disc electrode setup was used for electrodeposition. Before electroplating, pretreatments are necessary to get rid of the impurities. And the pretreatment procedure of substrates can be shown in Fig.2 (rinsing samples with de-ionized water).

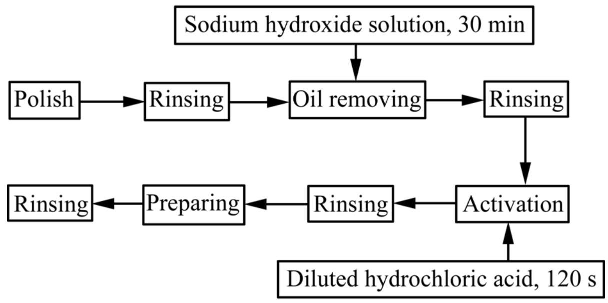

Fig.2 Technical flow chart of electrodeposited plating

Specimens were prepared under the same fabrication conditions of electrodeposition. Fig.3 shows the shape and size of tensile specimen. Then the tensile test was performed at a nominal rate of 0.1 mm/s using an Instron system at room temperature.

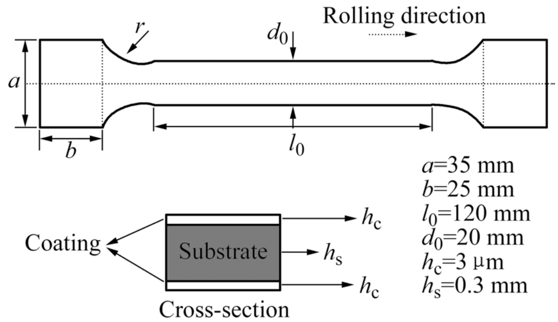

Fig.3 Shape and size of tension samples

3.2 Surface morphology and deformation texture of coatings

Philips Sirion 200 field emission scanning electron microscope (SEM), Hitachi S-520 SEM were used to show the surface morphology of nickel coatings. After tensile testing, deformation texture analysis was performed on a Bruker-AXS D500S theta-theta X-ray diffractometer with a diffracted beam graphite monochromator, using Cu K_{α} radiation. 2θ is 20°−90° with a step size of 0.01°.

3.3 Nano-indentation procedure

The nano-indentation measurements on nickel coating specimens shown in this work were performed using a TriboIndenter from Hysitron Inc with a three-sided pyramidal Berkovich diamond indenter. The load and displacement resolutions of the machine are 100 nN and 0.1 nm respectively. The loading and unloading rate $\mathrm{d}P/\mathrm{d}t$ of the indentation force P was 200 mN/s. In order to study material creep, a 5 s pause time was used between loading and unloading cycles. In all cases, at least 5 measurements were done at a certain load and averaged. A minimum of five experiments were performed in every load. From the load—displacement data, the values of elastic modulus and hardness of the deformation nickel coatings were calculated.

4 Results and discussion

4.1 Surface morphology and deformation texture

Fig.4 shows the surface morphologies of nickel coating before and after tensile deformation. From Fig.4 (a) it can be seen that the surface is not very smooth but no pinhole or microcrack is found and the surface is composed of gibbous part (position X) and flat-base part (position Y). With the increase of the tensile strain in the coating, the surface roughness increases and the microcrack is found in Fig.4 (b).

The texture composition of Ni coatings under the strain of 10% was investigated using XRD. As can be seen from Fig.5, Ni peaks indexed as (111), (200) and (220), at angles of 44.55°, 51.89° and 76.45° in the plot, match closely with listed values for fcc Ni peaks in XRD data tables. However, the textures Fe (200) and (211) do not exist in the nickel coating but the lower carbon steel sheet. After the tensile strain is larger than 10%, no new texture component can be found; however, the intensity of the every texture components changes in Fig.5. It is found that the intensity of Ni (111) decreases obviously but all the others change a bit when ε is 10%.

4.2 Mechanism of nickel coating

In order to fully investigate the mechanism of Ni coatings, an investigation of the coatings was carried out by nano-indentation. First the load—displacement curves were analyzed and certain information from these curves was ascertained. Then, the hardness and the elastic modulus were obtained via the Oliver and Pharr method. Fig.6 shows the load—displacement curves obtained for samples before and after tensile deformation at peak force of 1 mN.

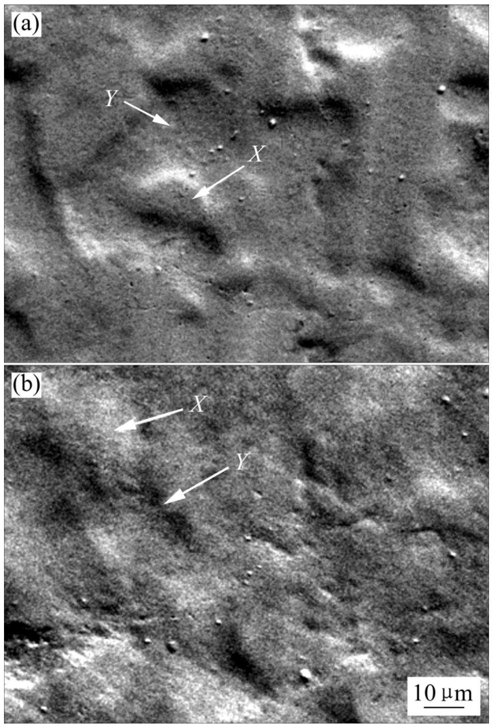

Fig.4 SEM images for (a) original electrodeposited Ni coating and (b) tensile Ni coating at strain of 10%

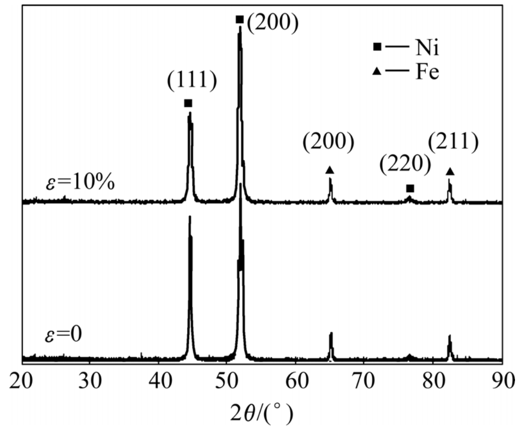

Fig.5 X-ray diffraction pattern for Ni coatings

In Fig.6, to the same maximum force $P_{\max}$ of 1 mN in the position X, the value 65.098 5 nm of the maximum depth $h_{\max}$ for the original electrodeposited sample is lower than 65.683 9 nm for the sample under strain of 10%. This shows that the hardness or stiffness of nickel coating decreases due to the strain ε is 10%. At the

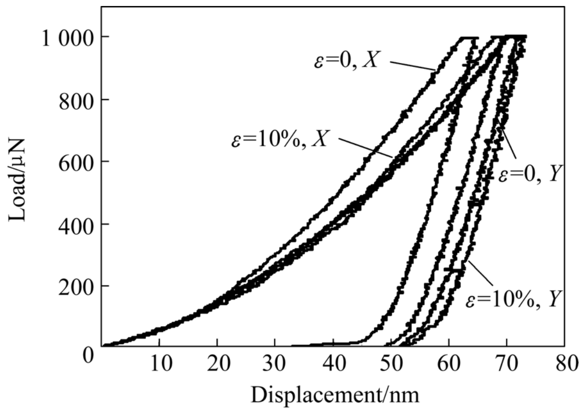

Fig.6 Load—displacement curves for nickel coatings at different positions

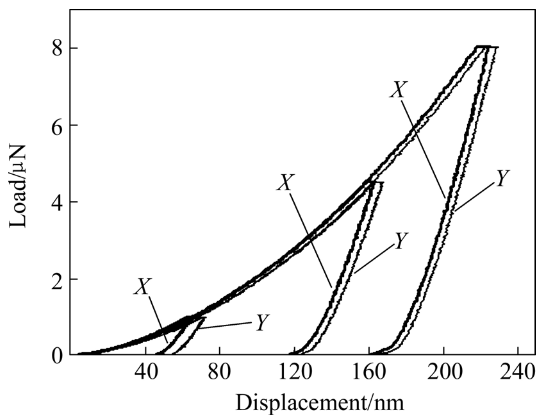

Fig.7 Load—displacement curves for original electrodeposited nickel coating at different positions and maximum applied force

position Y, the same case appears in the samples before and after tension. The results of hardness and elastic modulus are listed in Table 1, and they are given for the two samples in different positions under the maximum applied force of 1 mN. From Table 1, it can be seen that the indentation depth increases and the values of hardness and elastic modulus decrease after tensile deformation.

Table 1 Hardness, elastic modulus and creep values for nickel coatings

ε/%	Position	h_{max}/nm	h_f/nm	H/GPa	E/GPa	Δh/nm
0	X	65.098	55.052	9.365	242.513	1.252
	Y	72.416	61.971	7.742	207.356	1.428
10	X	65.683	55.349	9.075	237.914	1.847
	Y	73.362	63.986	7.335	230.717	1.982

During the pause at maximum load, the displacement is seen to increase due to creep [11−12]. Indentation creep was studied by a number of researchers [13−18]. In this work, the creep value Δh at position X increases to 1.847 nm for the sample after tensile deformation from 1.252 nm for the original electrodeposited sample during the pause 5 s in Table 1. This shows that tensile deformation leads to the increase of the creep value.

Fig.7 shows the load—displacement curve for the original electrodeposited nickel coating under different applied forces 1.0, 4.5 and 8.0 mN at the positions X and Y, respectively.

It can be seen that the indentation depth increases with the increase of force and these curves are fitted to the following equation:

$$P = Ch^2$$

In addition, all unloading curves are parallel, which shows that the elastic-plastic property is nearly the same in the nickel coating here and there.

Figs.8 (a) and (b) show the atomic force microphotographs at the maximum applied force of 8 mN for the nickel coatings before and after tensile deformation, respectively. From the two figures it can be concluded that the indentation area increases obviously after the tensile deformation of 10%. The reason is also that the values of hardness and elastic modulus decrease.

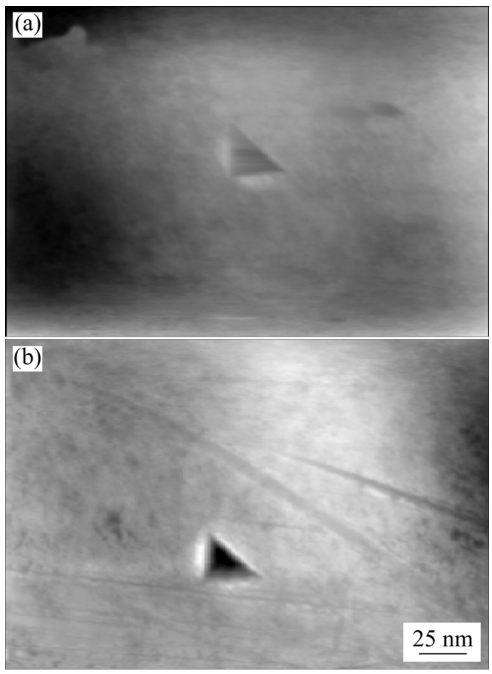

Fig.8 Atomic force microphotographs at maximum applied force of 8.0 mN for nickel coatings at different strains: (a) 0; (b) 10%

5 Conclusions

1) After deformation, there is no new texture for nickel coatings, but the change of the intensity of the deformation textures exists, especially the Ni (111)

decreases largely.

2) The indentation depths increase with the tensile strain ε=10%. Due to the increase of depth, the hardness and elastic modulus both decrease.

3) After tensile deformation in the coating, the surface roughness increases and the microcrack is found.

References

[1] BUDROVIC Z, SWYGENHOVEN H V. Plastic deformation with reversible peak broadening in nanocrystalline nickel[J]. Science, 2004, 304(1): 9−11.

[2] WANG G F, CHAN K C, ZHANG K F. Low temperature superplasticity of nanocrystalline electro-deposited Ni-Co alloy [J]. Scripta Materialia, 2006, 54(3): 765−770.

[3] TJONG S C, CHEN H. Nanocrystalline materials and coatings [J]. Material Science and Engineering R, 2004, 45(1): 1−88.

[4] MARDER A R. The metallurgy of zinc-coated steel[J]. Progress in Materials Science, 2000, 45(1): 191−271.

[5] LONG S G, ZHOU Y C, PAN Y. Computation of deformation-induced textures in electrodeposited nickel coating [J]. Trans Nonferrous Met Soc China, 2006, 16(1): s232−s238.

[6] ZHOU L Q, ZHOU Y C, PAN Y. Coating thickness variation during multistep drawing processes [J]. Journal of Materials Science Letter, 2004, 39(2): 757−760.

[7] CHOWDHURY S, LAUGIER M T, RAHMAN I Z. Measurement of the mechanical of carbon nitride thin films from the nanoindentation loading cure [J]. Diamond and Related Materials, 2004, 13(4/8): 1543−1548.

[8] PETHICA J B, HUNTCHINGS R, OLIVER W C. Hardness measurements at penetration depths as small as 20 nm [J]. Philosophical Magazine A, 1983, 48(4): 593−606.

[9] DOERNER M F, NIX W D. A method for interpreting the data from depth-sensing indentation instruments [J]. J Mater Research, 1986, 1(4): 601−609.

[10] BRISCOE B J, SEBASTIAN K S, SINHA S K. Application of the compliance method to microhardness measurements of organic polymers [J]. Philosophical Magazine A, l996, 74(19): 1159−1169.

[11] WANG F, XU K. An investigation of nanoindentation creep in polycrystalline Cu thin film [J]. Materials Letter, 2004, 58(11): 2345−2349.

[12] FISCHER-CRIPPS A C. A simple phenomenological approach to nanoindentation creep [J]. Materials Science and Engineering A, 2004, 385(2): 74−82.

[13] LUCUS B N, OLIVER W C. Indentation power law creep of high purity indium [J]. Metallurgical and Materials Transactions, 1999, 30(3): 601−610.

[14] YODER K B, ELMUSTAFA A A, LIN J C. Activation analysis of deformation in evaporated molybdenum thin films [J]. J Phys D: Appl Phys, 2003, 36(3): 884−895.

[15] FUJIWARA M, OTSUKA M. Indentation creep of b-Sn and Sn–Pb eutectic alloy [J]. Materials Science and Engineering A, 2001, 319/321(2): 929−933.

[16] YUE Z F, PROBST-HEIN M, EGGELER G. Determination of creep parameters from indentation creep experiments: A parametric study for single phase materials [J]. Mater High Temp, 2000, 17(4): 449−456.

[17] YUE Z F, EGGELER G, STOCKHERT B. A creep finite element analysis of indentation creep testing in two phase microstructures (particle/matrix- and thin film/substrate-systems) [J]. Computational Materials Science, 2001, 21(1): 37−56.

[18] DOMER D, ROLLER K, SKROTZKI B. Creep of a TiAl alloy: A comparison of indentation and tensile testing [J]. Materials Science and Engineering A, 2003, 357(1): 346−354.

(Edited by CHEN Can-hua)